HHS Public Access

Author manuscript

Nat Commun. Author manuscript; available in PMC 2014 December 20.

Published in final edited form as:

Nat Commun. ; 5: 4233. doi:10.1038/ncomms5233.

Hepatoprotective role of Sestrin2 against chronic ER stress

Hwan-Woo Park[1], **Haeli Park**[1], **Seung-Hyun Ro**[1], **Insook Jang**[1], **Ian A. Semple**[1], **David N. Kim**[1], **Myungjin Kim**[1], **Myeongjin Nam**[1,2], **Deqiang Zhang**[1], **Lei Yin**[1], and **Jun Hee Lee**[1,*]

[1]Department of Molecular and Integrative Physiology, University of Michigan, Ann Arbor, MI 48109, USA

[2]Department of Biological Science, Gachon University of Medicine and Science, Yeonsugu, Incheon 406-799, Republic of Korea

Abstract

Upon prolonged endoplasmic reticulum (ER) stress, cells attenuate protein translation to prevent accumulation of unfolded proteins. Here we show that Sestrin2 is critical for this process. Sestrin2 expression is induced by an ER stress-activated transcription factor CCAAT-enhancer-binding protein beta (c/EBPβ). Once induced, Sestrin2 halts protein synthesis by inhibiting mammalian target of rapamycin complex 1 (mTORC1). As Sestrin2-deficient cells continue to translate a large amount of proteins during ER stress, they are highly susceptible to ER stress-associated cell death. Accordingly, dietary or genetically-induced obesity, which does not lead to any pathological indication other than simple fat accumulation in liver of WT mice, can provoke Sestrin2-deficient mice to develop severe ER stress-associated liver pathologies such as extensive liver damage, steatohepatitis and fibrosis. These pathologies are suppressed by liver-specific Sestrin2 reconstitution, mTORC1 inhibition or chemical chaperone administration. The Sestrin2-mediated unfolded protein response (UPR) may be a general protective mechanism against ER stress-associated diseases.

Introduction

Excessive hepatic fat accumulation during obesity and non-alcoholic fatty liver disease (NAFLD) can induce chronic endoplasmic reticulum (ER) stress, a perturbation in ER homeostasis that can lead to hepatocyte death and a subsequent series of liver inflammation, oxidative stress accumulation and fibrosis collectively known as non-alcoholic steatohepatitis (NASH)[1, 2]. However, the progression from simple hepatosteatosis to NASH does not occur rapidly in most experimental models and human clinical cases of obesity. For

*Correspondence: Department of Molecular and Integrative Physiology, University of Michigan, Ann Arbor, MI 48109, USA. leeju@umich.edu.

Author Contributions H.W.P and J.H.L. designed experiments and analyzed data. H.W.P. performed cell culture experiments. D.Z. and L.Y. assisted with primary cell culture. H.W.P., H.L.P., I.J. and J.H.L. performed animal experiments. I.S. and D.N.K. assisted with protein analyses. I.J. and M.K. assisted with histological procedures. S.H.R. and M.N. assisted with mRNA expression analyses. H.W.P., H.L.P. and J.H.L. wrote the paper.

Author Information The authors declare no competing financial interests.

example, although overnutrition in rodents, caused by high fat diet (HFD) feeding or leptin deficiency, can result in obesity and hepatosteatosis, it does not spontaneously provoke steatohepatitis or fibrosis without further liver injury[3, 4]. In humans, a substantial portion of the population with obesity and hepatosteatosis shows fairly stable NAFLD symptoms for a prolonged period without progressing to NASH[5]. This attenuation of NASH development can be due to the existence of protective mechanisms that suppress obesity-associated ER stress.

A mechanism that protects cells against ER stress is generally defined as unfolded protein response (UPR)[6]. Perturbation of ER homeostasis leads to activation of three transmembrane ER stress sensor molecules: protein kinase RNA-like ER kinase (PERK), inositol-requiring enzyme 1 (IRE1) and activating transcription factor 6 (ATF6). These ER stress sensors together initiate protective UPR that increases molecular chaperone levels, attenuates protein synthesis and ER protein loading and upregulates ER-associated protein degradation and ER membrane biosynthesis. However, persistent and robust ER stress that exceeds the capacity of protective UPR may lead to cell death through apoptotic signaling activation[7] or ATP depletion[8]. The failure in protective UPR and the subsequent induction of ER stress-induced cell death are detrimental to physiological homeostasis, and these damages have been implicated in diverse degenerative diseases associated with obesity[9]. However, the detailed molecular mechanisms underlying the protective UPR have not been completely understood yet.

Sestrins are a family of stress-inducible proteins that can suppress mammalian target of rapamycin complex 1 (mTORC1) through activation of AMP-activated protein kinase (AMPK)[10, 11]. Sestrins are necessary for maintaining metabolic homeostasis and preventing age- and obesity-associated pathologies[11, 12, 13]. Among the three Sestrin homologues in mammals (Sestrin1-3), we recently found that, through unknown mechanisms, Sestrin2 expression in liver becomes elevated upon hypernutrition and obesity and functions to alleviate insulin resistance and hepatosteatosis[12]. Here we show that Sestrin2 is transcriptionally induced through the PERK-c/EBPβ pathway upon obesity-associated ER stress and maintains hepatic ER homeostasis by suppressing mTORC1-dependent protein translation. Correspondingly, loss of *Sesn2* allows for persistent protein synthesis in hepatocytes even under chronic ER stress, which further exacerbates the level of ER stress and subsequently results in extensive NASH-like pathologies such as liver damage, inflammation and fibrosis. Our results suggest that Sestrin2 critically mediates hepatocellular adaptation to ER stress and that Sestrin2 is the endogenous attenuator of NAFLD progression that operates primarily through maintaining ER homeostasis.

Results

Induction of Sestrin2 expression by ER stress insults

To understand how Sestrin2 expression is induced upon obesity, we subjected the human HepG2 cells to a series of culture environments that could mimic the conditions during obesity. As a result, we found that saturated fatty acids (SFA) such as palmitic acid (PA) or stearic acid (SA) induced prominent accumulation of Sestrin2 mRNA and protein (Fig. 1a-c and Supplementary Fig. 1a). In contrast, unsaturated fatty acids (UFA) such as oleic acid

(OA) or docosahexaenoic acid (DHA) not only failed to induce this upregulation (Supplementary Fig. 1b,c) but actually suppressed the effect of SFA (Supplementary Fig. 1d,e). Interestingly, the patterns of Sestrin2 expression were almost entirely correlated with the patterns of ER stress signaling activation that was monitored by PERK phosphorylation, c/EBP homologous protein (CHOP) expression and X-box binding protein 1 (XBP1) splicing (Fig. 1a and Supplementary Fig. 1a-e). Chemical ER stress inducers such as tunicamycin (Tm) or thapsigargin (Tg) also induced Sestrin2 expression in HepG2 cells (Supplementary Fig. 1f,g) and mouse liver (Supplementary Fig. 1h).

Obesity induces Sestrin2 through ER stress signaling

Overexpression of sarco-ER calcium pump 2b (SERCA2b) or administration of a chemical chaperone tauroursodeoxycholic acid (TUDCA), either of which can substantially reduce hepatic ER stress[14, 15, 16], was able to halt Sestrin2 induction caused by SFA (Fig. 1d,e; in HepG2 cells) or HFD-induced obesity (Fig. 1f,g and Supplementary Fig. 1i-k; in mouse liver). On the contrary, other known regulators of the Sestrin-family gene expression, such as oxidative stress, c-Jun N-terminal kinase (JNK), p53 or mTORC1, were not involved in Sestrin2 induction during obesity; antioxidants, SP600125, p53-shRNA and rapamycin all failed to suppress SFA- or obesity-induced Sestrin2 expression (Supplementary Fig. 1l-x). Thus, we concluded that obesity increases Sestrin2 expression primarily through activation of ER stress signaling.

PERK-c/EBPβ axis is responsible for Sestrin2 induction upon ER stress

We next searched for a molecular mechanism by which the ER stress signal could be sensed and transmitted to induce Sestrin2 expression upon obesity. Inhibition of an ER stress sensor PERK, but not that of the other two sensors IRE1 and ATF6, abolished the ability of SFA to induce Sestrin2 (Fig. 1h and Supplementary Fig. 2a,b). ATF4 and CHOP, the two most well-characterized transcription factors downstream of PERK[6], were not involved in SFA-induced Sestrin2 expression (Supplementary Fig. 2c,d), whereas c/EBPβ, another transcription factor downstream of PERK[17, 18] whose active isoform (LAP) accumulates inside the nucleus (Supplementary Fig. 2e,f) and binds to the *Sesn2* promoter upon ER stress insults (Fig. 1i,j and Supplementary Fig. 2g,h), was both necessary and sufficient to induce SFA- or obesity-induced Sestrin2 expression (Fig. 1k-n). These results indicate that the PERK-c/EBPβ signaling pathway controls Sestrin2 expression during obesity-associated ER stress.

Sestrin2 links ER stress and AMPK-mTORC1 regulation

Several recent studies indicate that chronic ER stress suppresses mTORC1 through an unknown mechanism that involves the activation of PERK and AMPK[19, 20]. Our findings here regarding the ER stress-induced Sestrin2 expression suggest that Sestrin2 may be the unknown moderator that bridges ER stress signaling and mTORC1 function. Indeed, Sestrin2-deficient cells and tissues could not activate AMPK or inhibit mTORC1 signaling upon SFA- (Fig. 2a-e) or Tm-induced ER stress (Fig. 2f-h). The signaling misregulation was not due to defects in energy homeostasis as cellular ATP levels were not significantly

altered by either Sestrin2 deficiency or ER stress insults (Fig. 2i,j). These results demonstrate that mTORC1 suppression during ER stress is dependent on Sestrin2.

Sestrin2 attenuates translation during chronic ER stress

Although PERK-mediated eukaryotic translation initiation factor 2α (eIF2α) phosphorylation can halt protein translation during the early phase of ER stress, this inhibitory effect is only temporary and quickly diminished during prolonged ER stress[6, 8]. Paradoxically, other ER stress signaling components downstream of PERK and eIF2α, such as ATF4 and CHOP, were found to increase protein synthesis and antagonize the effect of eIF2α phosphorylation[8]. Considering that mTORC1 is a major regulator of protein translation, Sestrin2-mediated mTORC1 suppression that occurs during ER stress may provide an alternative explanation for the inhibition of protein translation. During the early phase of ER stress (within 3 hr of SFA treatment), Sestrin2-deficient cells properly ceased protein translation like control cells (Supplementary Fig. 3a,b). However, after 9 hr of SFA-induced ER stress, Sestrin2-deficient HepG2 cells and mouse primary hepatocytes continued to translate large amounts of proteins while control cells managed to cease protein synthesis under the same condition (Fig. 2k-n and Supplementary Fig. 3a-c), suggesting that Sestrin2 is indeed critical for protein synthesis regulation during chronic ER stress. Similarly, *Sesn2*$^{-/-}$ mice could not downregulate hepatic protein synthesis upon 24 hr of Tm treatment or 2 months of HFD feeding (Fig. 2o-r and Supplementary Fig. 3d-g) in contrast to WT mice[8, 15]. On the other hand, mTORC1 inhibition by Sestrin2 overexpression or rapamycin treatment was sufficient to suppress protein translation (Supplementary Fig. 3h,i) without inducing eIF2α phosphorylation or ATF4 expression (Supplementary Fig. 3j,k). Therefore, Sestrin2 is a critical mediator of UPR that halts mTORC1-dependent protein translation during chronic ER stress.

Sestrin2 deficiency aggravates ER stress during obesity

Cessation of protein translation is critical for decreasing ER protein load and preventing accumulation of unfolded proteins. Thus, we were curious if Sestrin2 was necessary for resolution of ER stress after insults. Sestrin2 deficiency strongly exacerbated SFA-induced ER stress in HepG2 cells and mouse primary hepatocytes, as evidenced by increased phosphorylation of PERK and eIF2α and upregulation of ER stress-induced gene expression (Supplementary Fig. 4a-d). *Sesn2*$^{-/-}$ mice also exhibited extensive aggravation of ER stress, either upon Tm treatment- (Fig. 3a,b and Supplementary Fig. 4e-g), HFD- (Fig. 3c-f and Supplementary Fig. 4h,i) or *Lep*^{ob} mutation-induced obesity (Fig. 3g-i and Supplementary Fig. 4j). Hyperactivated ER stress signaling in obese *Sesn2*$^{-/-}$ mouse liver was completely suppressed by liver-specific transduction of Sestrin2 (Supplementary Fig. 5a-d), suggesting that Sestrin2 suppresses hepatic ER stress in a tissue-autonomous manner.

Sestrin2 controls ER homeostasis through AMPK-mTORC1

Sestrin2 has two independent biological activities largely divided into regulating the AMPK-mTORC1 signaling and suppressing the reactive oxygen species accumulation[11]. We found that, in Sestrin2-silenced cells, ER stress was strongly reduced by aminoimidazole carboxamide ribonucleotide (AICAR, an activator of AMPK) and rapamycin as well as by

another mTORC1 inhibitor PP242 and a translation inhibitor cycloheximide (CHX) (Fig. 4a-c and Supplementary Fig. 6a,b), while treatment of antioxidants such as BHA and N-acetylcysteine (NAC) turned out to be ineffective (Fig. 4b,c). Inhibition of mTORC1 by RaptorshRNA also ameliorated excessive ER stress signaling in Sestrin2-deficient cells (Fig. 4d,e), while mTORC1 activation by TSC2-shRNA exacerbated PA-induced ER stress (Fig. 4f,g). In liver of obese *Sesn2*$^{-/-}$ mice, liver-specific AMPK^{CA} transduction or systemic AICAR administration was sufficient to suppress ER stress signaling (Fig. 4h-k and Supplementary Fig. 6c,d). Consistent with the known roles of mTORC1 in regulating protein translation, AICAR, rapamycin and cycloheximide all suppressed protein translation in SFA-treated Sestrin2-deficient cells (Supplementary Fig. 6e,f), whereas TSC2 inhibition upregulated protein synthesis in SFA-treated control cells (Supplementary Fig. 6g,h). We also tested whether alleviation of protein synthesis through the eIF2a pathway could reduce ER stress in *Sesn2*$^{-/-}$ mice. Salubrinal, a specific inhibitor of eIF2α dephosphorylation[21] (Supplementary Fig. 7a,b), substantially suppressed ER stress in livers of *Sesn2*$^{-/-}$ mice (Supplementary Fig. 7c-e). Taken together, our findings indicate that Sestrin2 maintains ER homeostasis primarily through regulation of the AMPK-mTORC1-protein synthesis signaling pathway.

Sestrin2 is required to prevent liver damage during obesity

Because excessive ER stress can result in cell death[7, 8], we examined if Sestrin2 is required for ensuring cell's viability during ER stress insults. Upon prolonged SFA treatment for 16-24 hr, Sestrin2-deficient HepG2 cells and mouse primary hepatocytes exhibited remarkably increased apoptotic cell death compared to control cells (Supplementary Fig. 8a-d), consistent with heightened ER stress level (Supplementary Fig. 4a-d). *Sesn2*$^{-/-}$ mouse liver, upon Tm-induced ER stress, also exhibited more severe liver damage manifested by ectopic hepatocyte apoptosis and substantial elevation in serum alanine aminotransferase (ALT) levels compared to WT mouse liver (Supplementary Fig. 8e-g). More strikingly, HFD- or *Lep*^{ob}-induced obesity, which by itself does not induce any liver damage in WT mice, provoked *Sesn2*$^{-/-}$ mice to exhibit extensive hepatocyte death (Fig. 5a,b) and prominently elevated ALT levels (Fig. 5c), both of which were completely resolved by liver-specific reconstitution of Sestrin2 (Fig. 5d-f). TUDCA and salubrinal also effectively suppressed liver damage of obese or Tm-treated *Sesn2*$^{-/-}$ mice (Fig. 5g-i and Supplementary Fig. 7f,g), suggesting that unresolved hepatic ER stress is the main cause of the liver damage observed. These data collectively highlight Sestrin2 as a critical hepatoprotective agent that prevents hepatocyte apoptosis and liver damage upon both acute and chronic ER stress.

Sestrin2 is an endogenous attenuator of steatohepatitis

We found that dying hepatocytes in liver of obese *Sesn2*$^{-/-}$ mice was frequently associated with aggregation of dense-nucleated cells (Supplementary Fig. 9a), most of which were identified as F4/80-positive macrophages (Supplementary Fig. 9b). Some of the aggregated macrophages were proliferative as judged from positive BrdU staining (Supplementary Fig. 9c). As a result, liver of obese *Sesn2*$^{-/-}$ mice accumulated a highly increased number of macrophages (Fig. 6a,b), and these characteristics clearly imply the occurrence of active steatohepatitis. The steatohepatitis phenotype was completely suppressed by liver-specific

Sestrin2 reconstitution (Fig 6c,d), TUDCA administration (Fig 6e,f) and AMPK reactivation (Fig. 6g,h). In addition, *Sesn2* loss also aggravated Tm-induced steatohepatitis (Supplementary Fig. 9d,e).

Sestrin2 deficiency provokes liver fibrosis in obese mice

Hepatocyte death and subsequent activation of liver inflammation can lead to activation of hepatic stellate cells (HSCs) that are known to secrete collagen. Although liver from obese WT mice only displayed a few activated HSCs, visualized by alpha-smooth muscle actin (α-SMA) staining, liver from obese *Sesn2*$^{-/-}$ mice contained a substantially increased number of activated HSCs (Supplementary Fig. 9f,g). Consistent with this finding, there was a significant increase in collagen deposition in liver from obese *Sesn2*$^{-/-}$ mice (Supplementary Fig. 9h,i), validating the occurrence of liver fibrosis. Extensive fibrosis observed in *Lep*$^{ob/ob}$/*Sesn2*$^{-/-}$ mouse liver was particularly striking because *Lep*$^{ob/ob}$ mutant mice were reported to be very resistant to liver fibrosis[3]. Taken together, these data collectively indicate that, during obesity, Sestrin2-mediated ER stress suppression is critical for preventing NASH-like liver pathologies including fibrosis (Fig. 6i,j).

Sestrin2 regulates metabolism through ER stress suppression

Persistent activation of ER stress signaling can provoke excessive fat accumulation and insulin resistance[14, 15]. Tm-induced liver fat accumulation became more prominent and persistent upon Sestrin2 deficiency (Supplementary Fig. 10a,b). Although neither Tm nor Sestrin2 deficiency significantly increased expression of genes responsible for hepatic lipogenesis (Supplementary Fig. 10c) as previously reported[12, 22], serum triglyceride level, which is usually decreased by Tm-induced ER stress[23], was even further lowered by loss of *Sesn2* (Supplementary Fig. 10d). The rapid reduction in plasma lipid level upon ER stress reflects defective secretion of lipoproteins from hepatocytes[23, 24], which also causes acute hepatosteatosis. These results raise a possibility that Sestrin2 may control liver metabolism through regulating ER homeostasis. Indeed, increased hepatosteatosis and hepatic insulin resistance phenotypes of obese *Sesn2*$^{-/-}$ mice (Fig. 7a-d)[12, 25] were strongly suppressed by liver-specific reconstitution of Sestrin2 (Fig. 7e-h) or TUDCA administration (Fig. 7i-l), either of which can prevent hepatic ER stress. Thus, Sestrin2-mediated suppression of hepatic ER stress is not only required to prevent liver damage but also critical for proper regulation of lipid and glucose homeostasis.

Discussion

Although Sestrin2 was originally identified as a protein inducible upon DNA damage and oxidative stress[26], these stress insults turned out to be not responsible for Sestrin2 upregulation during obesity. Rather, disruption of ER homeostasis was the critical event responsible for obesity-induced Sestrin2 expression. An ER stress sensor PERK and its downstream transcription factor c/EBPβ play essential roles in Sestrin2 upregulation upon nutritionally- or chemically-induced ER stress. Other signaling mediators of ER stress, such as IRE1, ATF6, ATF4, CHOP and JNK, appeared not to be significantly involved in this process. Because Sestrin2 is the only Sestrin-family protein inducible upon obesity or ER stress, loss of *Sesn2* was not compensated by the presence of Sestrin1 or Sestrin3. This

allowed us to investigate the physiological functions of Sestrin2 in the context of ER stress using Sestrin2-deficient cells and mice.

Sestrin2-deficient cells cannot cease protein translation upon prolonged ER stress insults even though they exhibit prominently elevated PERK-eIF2α signaling activities. This finding was particularly striking to us because it has been formerly believed that ER stress-induced translation arrest is solely and directly mediated by PERK-dependent phosphorylation of eIF2α[6]. However, according to our results, Sestrin2-mediated mTORC1 regulation can be another important mechanism that can suppress protein translation during ER stress. Because Sestrin2-deficient cells lack this mechanism, they exhibited excessive ER stress that induces activation of the PERK-eIF2α signaling as well as the other branches of ER stress signaling. Increased ER stress observed in Sestrin2-deficient cells was suppressible by genetic or pharmacological inhibition of mTORC1. Therefore, Sestrin2-mediated mTORC1 regulation is an important UPR mechanism downstream of the PERK-eIF2α-c/EBPβ signaling that prevents excessive accumulation of unfolded proteins and aggravation of ER stress (Fig. 6i,j).

Recent reports have shown that deregulation of mTORC1 or protein translation can promote accumulation of unfolded and misfolded proteins, thereby further sensitizing cells to ER stress insults[27, 28, 29]. Consistent with these, Sestrin2-deficient hepatocytes were hyper-susceptible to ER stress-induced cell death, and *Sesn2*$^{-/-}$ mice were prone to develop ER stress-induced liver pathologies associated with hepatocyte death. The liver pathologies were suppressed by either AICAR or TUDCA administration, suggesting that defective AMPK-mTORC1 regulation and subsequent exacerbation of ER stress are the causes of these pathologies.

In summary, we have described a role for Sestrin2 as the critical component of hepatic UPR that mediates ER stress-induced suppression of protein synthesis. Sestrin2-mediated UPR mechanism is important for suppression of obesity-associated NAFLD pathologies including liver damage and steatohepatitis as well as fat accumulation and insulin resistance. Sestrin2's protective role against ER stress may be also important in other non-hepatic tissues that may experience increased levels of ER stress during obesity. Considering that unresolved ER stress is a possible pathogenetic cause of diverse diseases including cancer, neurodegeneration, type 1/2 diabetes and atherosclerosis[9] and that obesity increases incidences of these degenerative diseases[30], it would be much of interest to investigate possible protective roles of Sestrin2 against progression of these degenerative diseases beyond the scope of liver pathologies.

Methods

Antibodies and Reagents

Antibodies against Sestrin1 and Sestrin2 were generated from bacterially-expressed recombinant proteins as described[12]. Antibodies against phospho-PERK (Cell Signaling, Santa Cruz), PERK (Cell Signaling, Santa Cruz) ATF4 (Santa Cruz), ATF6 (Santa Cruz), c/EBPβ (Santa Cruz), RNA polymerase II (Santa Cruz), SERCA2 (Santa Cruz), phospho-S6 kinase (p-S6K; Cell Signaling, Santa Cruz), S6K (Santa Cruz), phospho-AMPKα (Santa

Cruz), AMPKα (Santa Cruz), CHOP (Cell Signaling, Santa Cruz), IRE1α (Santa Cruz), heavy chain-binding protein (BiP; Cell Signaling), protein disulfide isomerase (PDI; Cell Signaling), phospho-JNK (Cell Signaling), JNK (BD Biosciences), p53 (Santa Cruz), phospho-c-Jun (Santa Cruz), c-Jun (Santa Cruz), phospho-S6 (Cell Signaling), S6 (Cell Signaling), phospho-eIF4E-binding protein (p-4E-BP; Cell Signaling), 4E-BP (Cell Signaling), phospho-eIF2α (Cell Signaling), eIF2α (Santa Cruz), Raptor (Cell Signaling), TSC2/tuberin (Santa Cruz), Sestrin2 (Proteintech), Sestrin3 (Abcam), F4/80 (Invitrogen), α-SMA (Abcam), Actin (DSHB), puromycin (DSHB) and Tubulin (Sigma) were used as primary antibodies. Horseradish peroxidase (HRP)-conjugated secondary antibodies (Bio-Rad), biotin-conjugated secondary antibodies (BD Biosciences), streptavidin-HRP (BD Biosciences) and Alexa Flour-conjugated secondary antibodies (Invitrogen) were used for immunoblotting and immunostaining procedures. Fatty acid free and low endotoxin BSA, palmitic acid, stearic acid, oleic acid, docosahexaenoic acid, tunicamycin, thapsigargin, insulin, glucose, Oil Red O, butylated hydroxyanisole, and N-acetyl cysteine were purchased from Sigma. Cycloheximide was from Amresco, and PP242 was from Chemdea. TUDCA was purchased from EMD Millipore. SP600125, rapamycin and AICAR were purchased from LC Labs. Salubrinal was purchased from Calbiochem.

Cell Culture

HepG2 cells (gift from Dr. Saltiel) were maintained in Dulbecco's modified Eagle's medium (DMEM, Invitrogen) containing 10% fetal bovine serum (FBS, Sigma), 50 U ml^{-1} penicillin and 50 mg ml^{-1} streptomycin. De-lipidated low-endotoxin BSA was loaded with indicated fatty acids and applied to cultured cells as described[31].

Mice and Diets

WT, *Sesn2*$^{-/-}$ and *Lep*$^{ob/ob}$ mice are in C57BL/6 background as described[12]. Male mice of indicated age were used for the study. Mice were maintained in filter-topped cages and were given free access to autoclaved regular chow diet (LFD) or HFD (composed of 59% fat, 15% protein, and 26% carbohydrates based on caloric content; Bio-Serv) and water at University of Michigan (UM) according to NIH and institutional guidelines. All animal studies were overseen by the University Committee on Use and Care of Animals (UCUCA) at UM.

Lentiviruses

The lentiviral plasmids for sh-Sestrin2[10], sh-p53[32], sh-c/EBPβ[33], sh-Raptor and sh-TSC2[12] were previously described. Lentiviral plasmids for sh-PERK (TRCN0000001401 and TRCN0000001399), sh-ATF6 (TRCN0000017853 and TRCN0000017855), sh-CHOP (TRCN0000007264) and sh-ATF4 (TRCN0000013575) were purchased from Open Biosystems (Huntsville, AL). Lentiviral IRE1α^{DN} construct was obtained from Addgene (Cambridge, MA). Lentiviruses were generated in the Vector Core facility at the UM.

Adenoviruses

Adenoviruses expressing AMPK^{CA} (Ad-AMPK^{CA}) were purchased from Eton Biosciences. Adenoviruses expressing the 2b isoform of SERCA2 (Ad-SERCA2b) were gifts from Dr.

Hotamisligil[15]. Adenoviruses expressing c/EBPβ and sh-c/EBPβ were gifts from Dr. Lin[34]. Control adenoviruses were supplied by the UM Vector Core. Adeno-associated viruses (AAV) for GFP (AAV-Con) and Sestrin2 (AAV-Sesn2) were gifts from Dr. Pura Munoz (UPF, Spain). The viruses were amplified in the UM Vector Core. For hepatic gene transfer, 10^9 plaque-forming units of viruses were injected into mice through tail vein.

Immunoblotting

Cells or tissues were lysed in RIPA buffer (50 mM Tris-Cl pH 7.4, 150 mM NaCl, 1% sodium deoxycholate, 1% NP-40; 0.1% SDS) or cell lysis buffer (20 mM Tris-Cl pH 7.5, 150 mM NaCl, 1 mM EDTA, 1 mM EGTA, 2.5 mM sodium pyrophosphate, 1 mM β-glycerophosphate, 1 mM Na_3VO_4, 1% Triton-X-100) containing protease inhibitor cocktail (Roche). After being clarified by centrifugation, lysates were boiled in SDS sample buffer, separated by SDS-PAGE, transferred to PVDF membranes and probed with the indicated antibodies. Primary antibody dilution factors were 1:200 (all Santa Cruz antibodies), 1:100 (anti-puromycin antibody) or 1:1000 (all other antibodies). After incubation with secondary antibodies conjugated with HRP (1:2000), chemiluminescence was detected and quantified using LAS4000 (GE) system. Full sized scans of all western blots are provided in Supplementary Fig. 11.

Quantitative reverse transcriptase/real time PCR (qRT-PCR)

Total RNA was extracted from tissues or cells using Trizol reagent (Invitrogen), and cDNA was made using MMLV-RT (Promega) and random hexamers (Invitrogen). Quantitative PCR was performed in a Real-Time PCR detection system (Applied Biosystems) with iQ™ SYBR Green Supermix (Bio-rad) and relevant primers. Relative mRNA expression was calculated form the comparative threshold cycle (Ct) values relative to Cyclophilin A (CypA). Primers for human Sestrin1-3[35], human CypA[36], human XBP1[37], mouse XBP1[38], active spliced form of mouse XBP1[38] and human XBP1[39], mouse BiP[40], mouse ER degradation-enhancing alpha-mannosidase-like 1 (Edem1)[40], mouse ER oxidoreductin-1α (Ero1α)[40], human CHOP[36], mouse CHOP[40], mouse PDI[41], mouse ER-localized DnaJ homologue 4 (ERdj4)[41], mouse HMG-CoA reductase (Hmgcr)[42], mouse sterol regulatory element-binding transcription factor 1 (Srebf1)[42], mouse Srebf2[42], mouse fatty acid synthase (Fasn)[43], mouse acetyl CoA carboxylase alpha (Acaca)[43], mouse Acacb[43], mouse β-Actin[44] and mouse CypA[12] were designed as described. The ratio of spliced (XBP1-s) to unspliced (XBP1-u) XBP1 levels was determined by semi-quantitative RTPCR; PCR products of XBP1-s and XBP1-u were separated by electrophoresis on a 2.5% agarose gel and visualized by ethidium bromide staining. Percent of XBP1 splicing was quantified using ImageJ (NIH).

Histology

Liver tissues were fixed in 10% buffered formalin, embedded in paraffin and stained with hematoxylin and eosin. To visualize collagen fibers, liver sections were stained with saturated picric acid containing 0.5% Sirius Red (Sigma). The sections were washed with distilled water, dehydrated, mounted and analyzed by light microscopy. For immunostaining of BiP, p-PERK and F4/80, paraffin-embedded liver sections were incubated with corresponding primary antibodies (1:200, 1:50 and 1:100, respectively), followed by

incubation with biotin-conjugated secondary antibodies (1:200) and streptavidin-HRP (1:300). The HRP activity was visualized by diaminobenzidine (DAB) staining. Hematoxylin counterstaining was applied to visualize nuclei. For α-SMA staining, liver sections were incubated with anti-α-SMA antibody (1:100), followed by incubation with Alexa Flour 594-conjugated secondary antibody (1:250) and counterstaining with DAPI (Invitrogen). TUNEL assay was performed using In Situ Cell Death Detection Kit-TMR-Red (Roche). Samples were analyzed under an epifluorescence-equipped light microscope (Olympus).

Glucose and insulin tolerance tests (GTT and ITT)

For GTT and ITT, mice fasted for 6 hr were injected with glucose (1 g per kg body weight i.p.) or insulin (0.65 U per kg body weight i.p.). Blood glucose was instantly measured at 0, 20, 40, 60, and 120 min after glucose or insulin injection using OneTouch Ultra glucose meter.

Oil Red O staining

OCT-embedded frozen liver sections were allowed to air dry and rinsed with 60% isopropanol, followed by staining with fresh 0.5% Oil Red O solution for 15 min. After staining, the slides were rinsed with 60% isopropanol, washed with distilled water, mounted and analyzed under light microscope (Olympus).

Serum ALT assay

Serum ALT levels were measured with an ALT activity assay kit (Sigma) according to the manufacturer's instructions.

ROS detection

Intracellular level of reactive oxygen species (ROS) was measured using ROS indicator chloromethyl-2′,7′-dichlorodihydrofluorescein diacetate (CM-H_2DCFDA, Invitrogen). Cells were treated with 5 μM CM-H_2DCFDA for 30 min at 37°C in the dark and washed in PBS, followed by observation under an epifluorescence-equipped microscope (Olympus). Dihydroxyethidium staining of liver tissues was done as described using freshly frozen sections[45].

Primary cell culture

Primary mouse hepatocytes were isolated from livers of 2-month-old lean WT or *Sesn2*$^{-/-}$ mice, as described[46].

Immunocytochemistry

For c/EBPβ staining, HepG2 cells were fixed with methanol and incubated with anti-c/EBPβ antibody (1:100), followed by incubation with Alexa Fluor 594-conjugated secondary antibody (1:500) and counterstaining with DAPI (Invitrogen). Samples were analyzed under an epifluorescence-equipped light microscope (Olympus).

Measurement of protein synthesis

To label newly synthesized proteins with L-azidohomoalanine (AHA) in cultured cells, cells were incubated with 25 μM AHA (Invitrogen) in methionine- and cysteine-free DMEM (Invitrogen) for 3 hr in the presence of 10% FBS and antibiotics. AHA-incorporated proteins were labeled with biotin using Click-iT Biotin Protein Analysis Detection Kit (Invitrogen). The biotin-labeled proteins were assayed by immunoblotting. To label newly synthesized proteins with AHA in mouse liver, mice were injected with 13 mg per kg body weight AHA (i.p.). After 15 min, liver was harvested and analyzed by Click-IT immunoblotting. To label nascent peptides with puromycin, cultured cells were incubated with 1 μM puromycin (Calbiochem) in normal culture medium, and mice were injected with 0.04 mmol per kg body weight puromycin (i.p.). After 30 min, cells and livers were harvested and puromycin-labeled proteins were detected by anti-puromycin immunoblotting.

Luciferase assay

The luciferase-based *Sesn2* reporter constructs and c/EBP^{DN} plasmid were described previously[47]. HepG2 cells were transfected with *Sesn2*-luciferase constructs and *renilla* luciferase expression vector (pTK-RL) by Lipofectamine 2000 (Invitrogen). After 48 hr, cells were treated with BSA or PA for 9 hr. Luciferase activity was analyzed using Dual-Luciferase reporter assay kit (Promega).

Chromatin immunoprecipitation (ChIP)

HepG2 cells were treated with BSA or PA for 9 hr and fixed with 1% paraformaldehyde for 10 min at room temperature. ChIP assays were performed using EZ-ChIP Kit (EMD Millipore) according to the manufacturer's instructions. Chromatin extracts were immunoprecipitated with anti-c/EBPβ or anti-RNA polymerase II antibodies. Protein-associated DNA was analyzed by quantitative PCR using the following primers targeting sequences between −278 and +13 bps from the transcription start site of *Sesn2* gene: 5′-TCCCTTTTCATCACGCAACC-3′ and 5′-CTCTGACACCAGCAGTTCAGC-3′.

Statistical Analysis

Statistical significance of differences between two groups was calculated by a two-tailed Student's t test. *P* values equal to or above 0.05 were considered not statistically significant (NS).

Supplementary Material

Refer to Web version on PubMed Central for supplementary material.

Acknowledgements

We thank Drs. M. Karin (UCSD), A.V. Budanov (VCU) and P. Munoz (UPF, Spain) for Sestrin-related reagents and their valuable comments. We also thank Drs. A. Saltiel, R.A. Miller, J. Lin, L. Rui, J.L. Guan, D. Lombard, S. Pletcher (UM), G.E. Hardingham (U of Edinburgh, UK), G. Hotamisligil (Harvard) and Santa Cruz Biotech Inc. for sharing cell lines, reagents and access to lab equipment. We thank Dr. Judith Connett for her critical reading of the manuscript. This work was supported by grants from the American Association for the Study of Liver Diseases/American Liver Foundation, American Diabetes Association (1-13-BS-106), Ellison Medical Foundation (AG-NS-0932-12) and NIH (P30-AG024824, P30-AG013283, P30-DK034933, P30-DK089503 and P30-CA046592).

References

1. Malhi H, Kaufman RJ. Endoplasmic reticulum stress in liver disease. J Hepatol. 2011; 54:795–809. [PubMed: 21145844]
2. Pagliassotti MJ. Endoplasmic reticulum stress in nonalcoholic fatty liver disease. Annu Rev Nutr. 2012; 32:17–33. [PubMed: 22809102]
3. Saxena NK, Ikeda K, Rockey DC, Friedman SL, Anania FA. Leptin in hepatic fibrosis: evidence for increased collagen production in stellate cells and lean littermates of ob/ob mice. Hepatology. 2002; 35:762–771. [PubMed: 11915021]
4. Wu J, et al. High dietary fat exacerbates arsenic-induced liver fibrosis in mice. Exp Biol Med (Maywood). 2008; 233:377–384. [PubMed: 18296743]
5. Angulo P. Nonalcoholic fatty liver disease. N Engl J Med. 2002; 346:1221–1231. [PubMed: 11961152]
6. Walter P, Ron D. The unfolded protein response: from stress pathway to homeostatic regulation. Science. 2011; 334:1081–1086. [PubMed: 22116877]
7. Szegezdi E, Logue SE, Gorman AM, Samali A. Mediators of endoplasmic reticulum stress-induced apoptosis. EMBO Rep. 2006; 7:880–885. [PubMed: 16953201]
8. Han J, et al. ER-stress-induced transcriptional regulation increases protein synthesis leading to cell death. Nat Cell Biol. 2013; 15:481–490. [PubMed: 23624402]
9. Marciniak SJ, Ron D. Endoplasmic reticulum stress signaling in disease. Physiological reviews. 2006; 86:1133–1149. [PubMed: 17015486]
10. Budanov AV, Karin M. p53 target genes sestrin1 and sestrin2 connect genotoxic stress and mTOR signaling. Cell. 2008; 134:451–460. [PubMed: 18692468]
11. Lee JH, Budanov AV, Karin M. Sestrins orchestrate cellular metabolism to attenuate aging. Cell Metab. 2013; 18:792–801. [PubMed: 24055102]
12. Lee JH, et al. Maintenance of metabolic homeostasis by Sestrin2 and Sestrin3. Cell Metab. 2012; 16:311–321. [PubMed: 22958918]
13. Lee JH, et al. Sestrin as a feedback inhibitor of TOR that prevents age-related pathologies. Science. 2010; 327:1223–1228. [PubMed: 20203043]
14. Ozcan U, et al. Chemical chaperones reduce ER stress and restore glucose homeostasis in a mouse model of type 2 diabetes. Science. 2006; 313:1137–1140. [PubMed: 16931765]
15. Fu S, et al. Aberrant lipid metabolism disrupts calcium homeostasis causing liver endoplasmic reticulum stress in obesity. Nature. 2011; 473:528–531. [PubMed: 21532591]
16. Park SW, Zhou Y, Lee J, Ozcan U. Sarco(endo)plasmic reticulum Ca2+-ATPase 2b is a major regulator of endoplasmic reticulum stress and glucose homeostasis in obesity. Proc Natl Acad Sci U S A. 2010; 107:19320–19325. [PubMed: 20974941]
17. Oyadomari S, Harding HP, Zhang Y, Oyadomari M, Ron D. Dephosphorylation of translation initiation factor 2alpha enhances glucose tolerance and attenuates hepatosteatosis in mice. Cell Metab. 2008; 7:520–532. [PubMed: 18522833]
18. Calkhoven CF, Muller C, Leutz A. Translational control of C/EBPalpha and C/EBPbeta isoform expression. Genes Dev. 2000; 14:1920–1932. [PubMed: 10921906]
19. Avivar-Valderas A, Bobrovnikova-Marjon E, Alan Diehl J, Bardeesy N, Debnath J, Aguirre-Ghiso JA. Regulation of autophagy during ECM detachment is linked to a selective inhibition of mTORC1 by PERK. Oncogene. 2013; 32:4932–4940. [PubMed: 23160380]
20. Appenzeller-Herzog C, Hall MN. Bidirectional crosstalk between endoplasmic reticulum stress and mTOR signaling. Trends Cell Biol. 2012; 22:274–282. [PubMed: 22444729]
21. Boyce M, et al. A selective inhibitor of eIF2alpha dephosphorylation protects cells from ER stress. Science. 2005; 307:935–939. [PubMed: 15705855]
22. Rutkowski DT, et al. UPR pathways combine to prevent hepatic steatosis caused by ER stress-mediated suppression of transcriptional master regulators. Dev Cell. 2008; 15:829–840. [PubMed: 19081072]
23. Zhang K, et al. The unfolded protein response transducer IRE1alpha prevents ER stress-induced hepatic steatosis. EMBO J. 2011; 30:1357–1375. [PubMed: 21407177]

24. Ota T, Gayet C, Ginsberg HN. Inhibition of apolipoprotein B100 secretion by lipid-induced hepatic endoplasmic reticulum stress in rodents. J Clin Invest. 2008; 118:316–332. [PubMed: 18060040]
25. Bae SH, et al. Sestrins activate Nrf2 by promoting p62-dependent autophagic degradation of Keap1 and prevent oxidative liver damage. Cell Metab. 2013; 17:73–84. [PubMed: 23274085]
26. Budanov AV, et al. Identification of a novel stress-responsive gene Hi95 involved in regulation of cell viability. Oncogene. 2002; 21:6017–6031. [PubMed: 12203114]
27. Young RM, et al. Dysregulated mTORC1 renders cells critically dependent on desaturated lipids for survival under tumor-like stress. Genes Dev. 2013; 27:1115–1131. [PubMed: 23699409]
28. Conn CS, Qian SB. Nutrient Signaling in Protein Homeostasis: An Increase in Quantity at the Expense of Quality. Sci Signal. 2013; 6:ra24. [PubMed: 23592839]
29. Ozcan U, et al. Loss of the tuberous sclerosis complex tumor suppressors triggers the unfolded protein response to regulate insulin signaling and apoptosis. Mol Cell. 2008; 29:541–551. [PubMed: 18342602]
30. Haslam DW, James WP. Obesity. Lancet. 2005; 366:1197–1209. [PubMed: 16198769]
31. Holzer RG, et al. Saturated fatty acids induce c-Src clustering within membrane subdomains, leading to JNK activation. Cell. 2011; 147:173–184. [PubMed: 21962514]
32. Sablina AA, Budanov AV, Ilyinskaya GV, Agapova LS, Kravchenko JE, Chumakov PM. The antioxidant function of the p53 tumor suppressor. Nat Med. 2005; 11:1306–1313. [PubMed: 16286925]
33. Gomis RR, Alarcon C, Nadal C, Van Poznak C, Massague J. C/EBPbeta at the core of the TGFbeta cytostatic response and its evasion in metastatic breast cancer cells. Cancer cell. 2006; 10:203–214. [PubMed: 16959612]
34. Ma D, Panda S, Lin JD. Temporal orchestration of circadian autophagy rhythm by C/EBPbeta. EMBO J. 2011; 30:4642–4651. [PubMed: 21897364]
35. Chen CC, et al. FoxOs inhibit mTORC1 and activate Akt by inducing the expression of Sestrin3 and Rictor. Dev Cell. 2010; 18:592–604. [PubMed: 20412774]
36. Meur G, et al. Insulin gene mutations resulting in early-onset diabetes: marked differences in clinical presentation, metabolic status, and pathogenic effect through endoplasmic reticulum retention. Diabetes. 2010; 59:653–661. [PubMed: 20007936]
37. Lin JH, et al. IRE1 signaling affects cell fate during the unfolded protein response. Science. 2007; 318:944–949. [PubMed: 17991856]
38. Sha H, et al. The IRE1alpha-XBP1 pathway of the unfolded protein response is required for adipogenesis. Cell metabolism. 2009; 9:556–564. [PubMed: 19490910]
39. van Schadewijk A, van't Wout EF, Stolk J, Hiemstra PS. A quantitative method for detection of spliced X-box binding protein-1 (XBP1) mRNA as a measure of endoplasmic reticulum (ER) stress. Cell Stress Chaperones. 2012; 17:275–279. [PubMed: 22038282]
40. Malhotra JD, et al. Antioxidants reduce endoplasmic reticulum stress and improve protein secretion. Proc Natl Acad Sci U S A. 2008; 105:18525–18530. [PubMed: 19011102]
41. Kawasaki N, Asada R, Saito A, Kanemoto S, Imaizumi K. Obesity-induced endoplasmic reticulum stress causes chronic inflammation in adipose tissue. Scientific reports. 2012; 2:799. [PubMed: 23150771]
42. Zhang W, et al. FoxO1 regulates multiple metabolic pathways in the liver: effects on gluconeogenic, glycolytic, and lipogenic gene expression. J Biol Chem. 2006; 281:10105–10117. [PubMed: 16492665]
43. Grefhorst A, et al. Differential effects of pharmacological liver X receptor activation on hepatic and peripheral insulin sensitivity in lean and ob/ob mice. Am J Physiol Endocrinol Metab. 2005; 289:E829–838. [PubMed: 15941783]
44. Fasshauer M, Klein J, Neumann S, Eszlinger M, Paschke R. Hormonal regulation of adiponectin gene expression in 3T3-L1 adipocytes. Biochemical and biophysical research communications. 2002; 290:1084–1089. [PubMed: 11798186]
45. Park EJ, et al. Dietary and genetic obesity promote liver inflammation and tumorigenesis by enhancing IL-6 and TNF expression. Cell. 2010; 140:197–208. [PubMed: 20141834]

46. Tong X, et al. Recruitment of histone methyltransferase G9a mediates transcriptional repression of Fgf21 gene by E4BP4 protein. J Biol Chem. 2013; 288:5417–5425. [PubMed: 23283977]

47. Papadia S, et al. Synaptic NMDA receptor activity boosts intrinsic antioxidant defenses. Nat Neurosci. 2008; 11:476–487. [PubMed: 18344994]

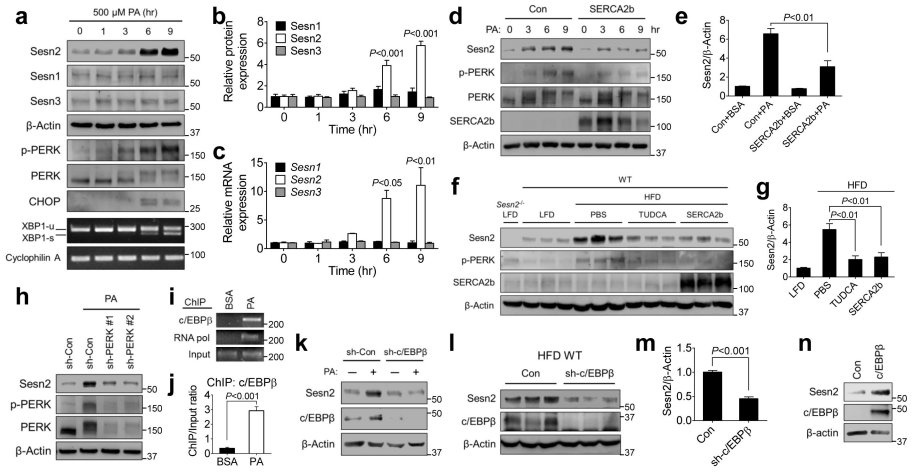

Figure 1. Obesity induces Sestrin2 through ER stress signaling

(**a-c**) HepG2 cells were treated with palmitic acid (PA) for indicated hr and analyzed by immunoblotting (images with black bands) and RT-PCR (images with white bands) (n = 3). P values were calculated between untreated (0 hr) and indicated groups (**b**,**c**). (**d**,**e**) At 48 hr after infection with GFP (Con)- or SERCA2b-overexpressing adenoviruses, cells were treated with BSA (0 hr) or PA for indicated hr (**d**) or 9 hr (**e**) (n = 3). (**f**,**g**,**l**,**m**) 6-month-old WT mice kept on LFD or HFD for 4 months were injected daily with vehicle (PBS) or TUDCA (500 mg per kg body weight i.p.) or transduced once with adenoviruses expressing SERCA2b, GFP (Con) or shRNA targeting c/EBPβ. After 10 days, livers were analyzed by immunoblotting (n = 3). (**h**,**k**) At 48 hr before PA treatment, cells were infected with lentiviruses expressing shRNAs targeting luciferase (Con), PERK (**h**) and c/EBPβ (**k**). After 9 hr of BSA (−) or PA treatment, cells were analyzed by immunoblotting. (**i**,**j**) Chromatin immunoprecipitation (ChIP) analysis of cells with indicated treatments (n = 3). (**n**) At 24 hr after infection with GFP (Con)- or c/EBPβ-overexpressing adenoviruses, cells were analyzed by immunoblotting. All data are shown as the mean ± s.e.m. P values are from Student's t test. Molecular weight markers are indicated in kDa (immunoblots) or bp (agarose gels).

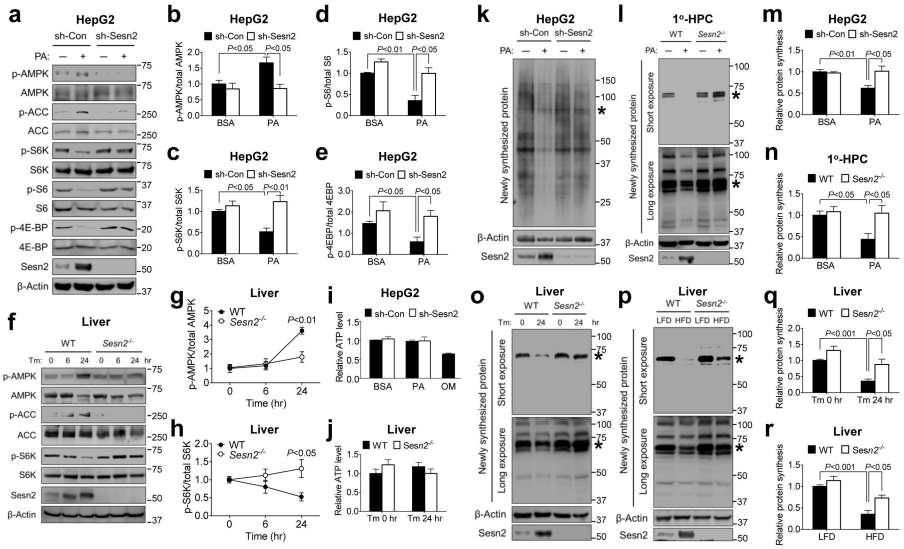

Figure 2. Sestrin2 suppresses mTORC1 and protein synthesis in response to ER stress

(**a-e**) At 48 hr after infection with shRNA lentiviruses for luciferase (Con) or Sestrin2, HepG2 cells were treated with PA for 9 hr and analyzed by immunoblotting (*n* = 3). AMPK signaling activity was monitored by phosphorylation of AMPK and acetyl-CoA carboxylase (ACC). mTORC1 signaling activity was monitored by phosphorylation of p70 ribosomal protein S6 kinase (S6K), ribosomal protein S6 and eIF4E-binding protein (4E-BP). (**f-h**) 2-month-old WT or *Sesn2*$^{-/-}$ mice kept on LFD were injected with tunicamycin (Tm, 500 mg per kg body weight i.p.). After indicated hr, livers were analyzed by immunoblotting (*n* = 4). (**i**,**j**) Relative intracellular ATP levels of indicated cells (**i**, *n* = 3) and liver tissues (**j**, *n* = 4). As a positive control for ATP depletion, HepG2 cells were treated with oligomycin (OM, 5 μg ml^{-1}) for 1 hr. (**k-r**) HepG2 cells transduced with sh-Con or sh-Sesn2 (**k**,**m**, *n* = 5) or primary hepatocytes (1°-HPC) isolated from WT or *Sesn2*$^{-/-}$ mice (**l**,**n**, *n* = 4) were treated with BSA (−) or PA for 9 hr. 2-month-old WT or *Sesn2*$^{-/-}$ mice were injected with Tm (**o**,**q**, *n* = 4) or kept on LFD or HFD for additional 2 months (**p**,**r**, *n* = 4). After indicated treatments, newly synthesized proteins in cells (**k-n**) and liver tissues (**o-r**) were visualized and quantified by Click-IT AHA® labeling system. The protein bands denoted by stars correspond to serum albumin (70kD), which is the most actively synthesized protein in normal hepatocytes. All data are shown as the mean ± s.e.m. *P* values are from Student's t test. Molecular weight markers are indicated in kDa.

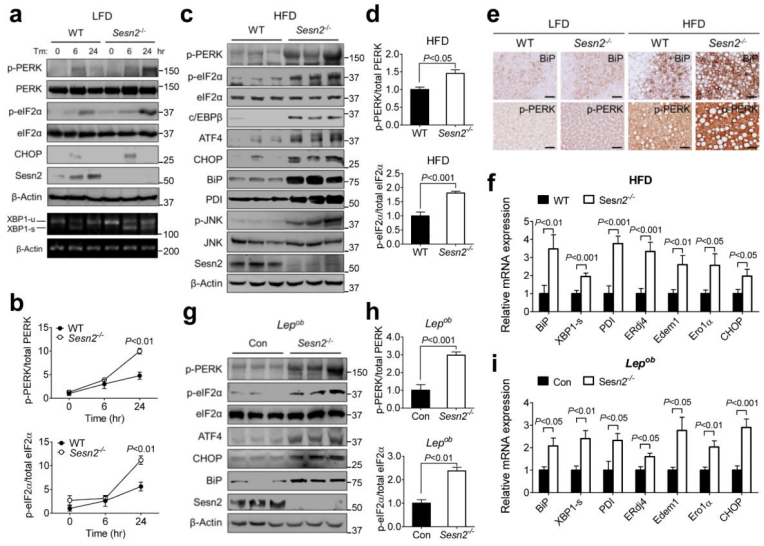

Figure 3. Sestrin2 deficiency exacerbates ER stress upon chemical insults or obesity

(**a**,**b**) 2-month-old WT or *Sesn2*$^{-/-}$ mice kept on LFD were injected with Tm (500 mg per kg body weight, i.p.). After indicated hr, livers were harvested from the treated mice and analyzed (n = 4). Protein phosphorylation and expression were analyzed by immunoblotting (images with black bands) (**a**) and quantified (**b**). XBP1 mRNA splicing was examined through semi-quantitative RT-PCR (images with white bands) (**a**). (**c**-**i**) 6-month-old WT (n = 6) and *Sesn2*$^{-/-}$ (n = 5) mice kept on LFD or HFD for 4 months (**c**-**f**) and 4-month-old *Lep*$^{ob/ob}$/*Sesn2*$^{+/-}$ (Con, n = 4) and *Lep*$^{ob/ob}$/*Sesn2*$^{-/-}$ (n = 6) mice kept on LFD (**g**-**i**) were analyzed. Protein phosphorylation and expression were analyzed by immunoblotting (**c**,**g**) and quantified by densitometry (**d**,**h**). Liver sections were stained with indicated antibodies (**e**). Relative mRNA expression of ER stress-inducible genes was quantified through qRT-PCR (**f**,**i**). Scale bars, 100 μm. All data are shown as the mean ± s.e.m. P values are from Student's t test. Molecular weight markers are indicated in kDa (immunoblots) or bp (agarose gels).

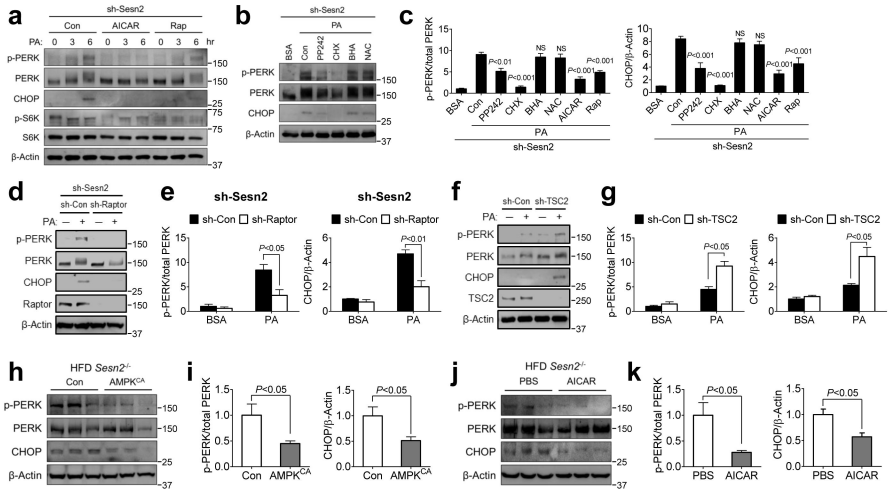

Figure 4. Sestrin2 controls ER homeostasis through the AMPK-mTORC1 axis

(**a**-**c**) HepG2 cells stably transduced with Sestrin2 shRNA (sh-Sesn2) were treated with PA for indicated hr (**a**) or 6 hr (**b**). PBS (Con), AICAR (1 mM), Rapamycin (Rap, 100 nM), PP242 (1 μM), cycloheximide (CHX, 180 μM), BHA (100 μM) and NAC (10 mM) were applied 1 hr before treating with PA. AICAR is an AMPK activator, PP242 is an mTOR inhibitor, and CHX is a protein translation inhibitor. Protein phosphorylation and expression were examined (**a**,**b**) and quantified (**c**) (n = 3). P values were calculated between PA+PBS (Con) and indicated groups. (**d**,**e**) Sestrin2-silenced HepG2 cells were transduced with shRNA lentiviruses for luciferase (Con) or Raptor (sh-Raptor). After 48 hr, cells were treated with BSA (−) or PA for 6 hr and analyzed by immunoblotting (n = 3). (**f**,**g**) At 48 hr after infection with shRNA lentiviruses for luciferase (Con) or TSC2 (sh-TSC2), HepG2 cells were treated with BSA (−) or PA for 6 hr and analyzed by immunoblotting (n = 3). (**h**-**k**) 5-month-old *Sesn2*$^{-/-}$ mice kept on HFD for 3 months were transduced once with adenoviruses expressing GFP (Con, n = 5) or constitutive active AMPK (AMPK^{CA}, n = 6) (**h**,**i**) or were injected daily with vehicle (PBS, n = 6) or AICAR (250 mg per kg body weight per day i.p., n = 5) (**j**,**k**). After 10 days, livers were harvested, and protein phosphorylation and expression were examined (**h**,**j**) and quantified (**i**,**k**). All data are shown as the mean ± s.e.m. P values are from Student's t test. Molecular weight markers are indicated in kDa.

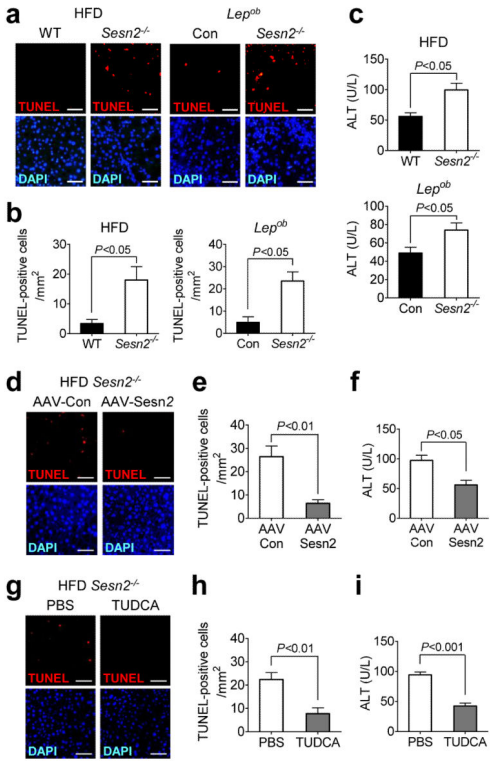

Figure 5. Sestrin2 prevents liver damage during obesity

(**a**-**c**) Livers and sera were collected from 6-month-old WT (n = 6) and $Sesn2^{-/-}$ (n = 5) mice kept on HFD for 4 months (HFD panels) or from 4-month-old $Lep^{ob/ob}/Sesn2^{+/-}$ (Con, n = 4) and $Lep^{ob/ob}/Sesn2^{-/-}$ (n = 6) mice kept on LFD (Lep^{ob} panels). Liver sections were subjected to TUNEL (red) and DAPI (blue) staining (**a**). TUNEL-positive cells were quantified (**b**). Serum ALT levels were quantified from indicated groups of mice (**c**). (**d**-**f**) Livers from obese $Sesn2^{-/-}$ mice transduced with AAV-Con (n = 4) or AAV-Sesn2 (n = 3) were subjected to TUNEL (red) and DAPI (blue) staining (**d**). TUNEL-positive cells in livers (**e**) and serum ALT levels (**f**) were quantified. (**g**-**i**) 5-month-old $Sesn2^{-/-}$ mice kept on HFD for 3 months were daily injected with vehicle (PBS, n = 4) or TUDCA (500 mg per kg body weight per day i.p., n = 5). After 10 days of the treatment, mice were sacrificed, and livers and sera were collected. Livers were subjected to TUNEL (red) and DAPI (blue) staining (**g**). TUNEL-positive cells in livers (**h**) and serum ALT levels (**i**) were quantified. Scale bars, 100 μm. All data are shown as the mean ± s.e.m. P values are from Student's t test.

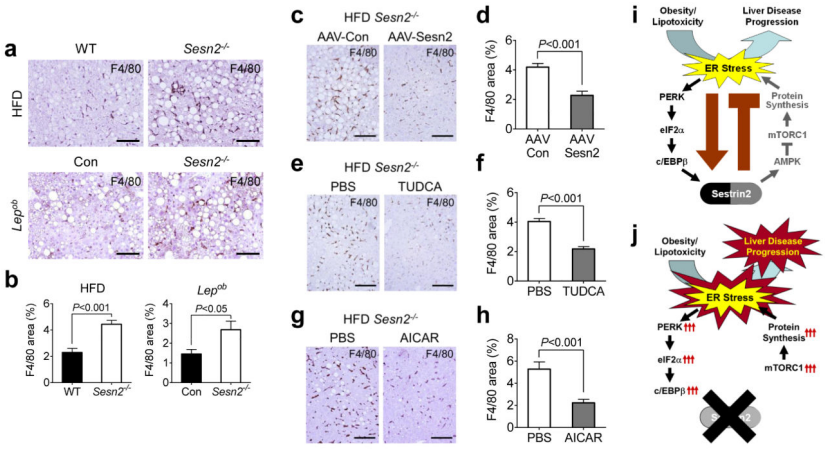

Figure 6. Sestrin2 is an endogenous attenuator of steatohepatitis progression

(**a**-**b**) Livers from WT and *Sesn2*$^{-/-}$ mice kept on HFD (HFD panels) or *Lep*$^{ob/ob}$/*Sesn2*$^{+/-}$ (Con) and *Lep*$^{ob/ob}$/*Sesn2*$^{-/-}$ mice kept on LFD (*Lep*^{ob} panels) were subjected to anti-F4/80 staining to visualize macrophage infiltration (**a**). F4/80-positive areas were quantified (**b**). (**c**-**h**) Livers from obese *Sesn2*$^{-/-}$ mice transduced with AAV-Con (n = 4) or AAV-Sesn2 (n = 3) (**c**,**d**) or injected with PBS (n = 4) or TUDCA (n = 5) (**e**,**f**) or PBS (n = 6) or AICAR (n = 5) (**g**,**h**) were analyzed by anti-F4/80 staining (**c**,**e**,**g**). F4/80-positive areas were quantified (**d**,**f**,**h**). Nuclei were visualized by hematoxylin (**a**,**c**,**e**,**g**). (**i**,**j**) Working model of how Sestrin2-mediated UPR attenuates NAFLD progression. In WT liver, Sestrin2 is induced during obesity through the PERK-c/EBPβ pathway to attenuate protein translation and thereby relieve ER stress (**i**). In *Sesn2*$^{-/-}$ liver, persistent mTORC1 activity elevates protein synthesis and subsequently aggravates ER stress, leading to facilitated NAFLD progression (**j**). Scale bars, 200 μm. All data are shown as the mean ± s.e.m. *P* values are from Student's t test.

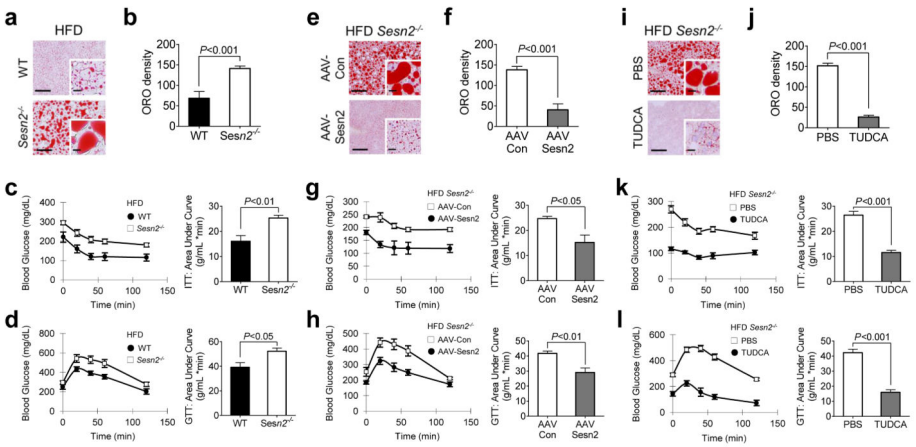

Figure 7. Sestrin2 controls liver metabolism through regulating ER homeostasis

(**a**-**d**) 6-month-old WT and *Sesn2*$^{-/-}$ mice were kept on HFD for 4 months. Livers were analyzed by Oil Red O (ORO) staining (**a**). ORO densities were quantified (**b**) (n = 4). Mice were tested for insulin resistance (ITT) (**c**) (n = 8) and for glucose tolerance (GTT) (**d**) (n = 8). Area-under-the-curve data for ITT (**c**) and GTT (**d**) were calculated. (**e**-**h**) 5-month-old *Sesn2*$^{-/-}$ mice kept on HFD for 3 months were transduced with AAV-Con (n = 4) or AAV-Sesn2 (n = 3). After 10 days, livers were harvested from the treated mice and analyzed by ORO staining (**e**). ORO densities were quantified (**f**). Mice were tested for insulin resistance at 5 days (**g**) and for glucose tolerance at 7 days (**h**) after AAV transduction. Area-under-the-curve data for ITT (**g**) and GTT (**h**) were calculated. (**i**-**l**) 5-month-old *Sesn2*$^{-/-}$ mice kept on HFD for 3 months were daily injected with vehicle (PBS, n = 4) or TUDCA (500 mg per kg body weight per day i.p., n = 5). After 10 days of treatment, livers were harvested from the treated mice and analyzed by ORO staining (**i**). ORO densities were quantified (**j**). Mice were tested for insulin resistance at 5 days (**k**) and for glucose tolerance at 7 days (**l**) after initiation of TUDCA treatment. Area-under-the-curve data for ITT (**k**) and GTT (**l**) were calculated. Scale bars, 200 μm; 10 μm (insets). All data are shown as the mean ± s.e.m. P values are from Student's t test.